Using Dimensionality Reduction to Create New Materials from Tabular BRDFs

Mislene da Silva Nunes
Universidade Federal de Sergipe
Departamento de Computação
Email: mislenesn@dcomp.ufs.br

Gastão Florêncio Miranda Junior
Universidade Federal de Sergipe
Departamento de Matemática
Email: gastao@mat.ufs.br

Beatriz Trinchão Andrade
Universidade Federal de Sergipe
Departamento de Computação
Email: beatriz@dcomp.ufs.br

***Abstract*—Representing reality in computer graphics requires simulating the appearance of real-world materials. Bidirectional Reflectance Distribution Functions (BRDFs) are commonly used to perform this task, as they represent the appearance of a material through the quotient between the reflected radiance and the incoming irradiance at this point. Acquiring the BRDF of a real material is an expensive task due to its high dimensionality, so strategies to take advantage of already existing measurements are a promising solution. In this paper we present an approach to create BRDFs for new materials from a basis of tabular representations of BRDFs. We apply dimensionality reduction in this basis and then we perform a triangulation in the resulting reduced space. Thus, any position in this reduced space can be used to create a new material: using the triangulation, we estimate coefficients that can be used to find the BRDF of this new material by interpolating materials in the original space. In addition, we present a technique to navigate in this reduced space that enables the creation of several different materials from two materials in the basis. This approach provides a wide range of new materials based on real measurements without the need to acquire new BRDFs. We show that our navigation is coherent and that it yields a smooth transition between materials.**

I. Introduction

In computer graphics, one of the factors that define the appearance of a material is the way it interacts with light under different settings. This interaction can be represented through Bidirectional Reflectance Distribution Functions (BRDFs). A BRDF is generally a function of the directions of incoming (ω_i) and reflected (ω_o) light (Figure 1), and describes the reflectance of a point on a surface through the quotient between the reflected radiance and the incoming irradiance at this point.

Different approaches can be used to characterize a real material through a BRDF. A material can be represented through a dense set of measurements, taken from different directions of incoming and exitant light. These samples are then stored as a tabular representation and retrieved when this material is rendered. Devices such as gonioreflectometers [2], [3] and image-based methods [4], [5] are used to perform this task. If the material is densely sampled, this representation is very detailed and represents the appearance of a material with high precision. However, collecting samples is a consuming task that demands storage space and generally requires long acquisition time.

Analytic models [6]–[10] are an alternative to the tabular BRDFs previously described. These models aim a compact representation of the appearance of materials at the cost of a potential loss in high frequency details. The formulation of these models is generally derived from the analysis of light behavior and from measured data.

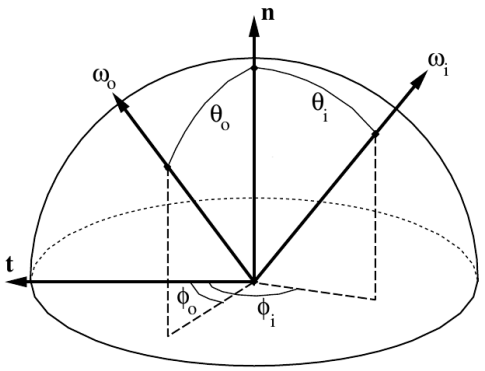

Fig. 1. Parameters of a BRDF: $\omega_i = (\theta_i, \phi_i)$ and $\omega_o = (\theta_o, \phi_o)$. The vector **n** is the surface normal; the vector **t** is the surface tangent. Figure extracted from Weyrich et al. [1].

Despite the cost that comes along with measuring real samples for a BRDF, tabular measurements provides BRDFs which are important computer graphics. Besides providing real measurements for research and analysis, it contributes to the creation of realistic images, representing real-world objects and scenes.

A solution proposed by researchers is to define a material through the combination of known BRDFs [11]–[14]. The materials can contain more details with accurate measurements and, as they are based on already existent measurements, present stable material behavior. In this paper, we present an approach to create unknown materials from a basis of BRDFs, aiming to provide a tabular representation of a new material without the need of measurements.

We use a basis of 100 materials composed of isotropic BRDFs at high resolution, acquired by Matusik et al. [5]. To create a new material, linear dimensionality reduction is applied in this basis using Principal Components Analysis (PCA). This way it is possible to generate a BRDF space, keeping it at a high resolution and at a compact representation. In addition, Delaunay triangulation is applied in this reduced space, to interpolate the materials using barycentric

coordinates. Thus, a new tabular representation of a BRDF is obtained through the interpolation of the materials in the original space, based on values provided by this compact and triangulated space.

Our approach creates new BRDFs from a basis of tabular representations of BRDFs, which can be synthetic or measured from real materials. The main contributions of this paper are:

- A compact representation strategy for a basis of tabular BRDFs;
- Tabular representations of BRDFs for new materials;
- A navigation strategy in the reduced space of BRDFs that enables the creation of different materials and illustrates the morphing of a material into another.

The new materials contribute to increase the variety of tabular BRDF representations that are required in computer graphics areas, such as realist rendering. Furthermore, a wide range of materials can be created according to the appearance desired by artists and product designers. They provide also a realism that is required in entertainment production.

II. Related Work

The acquisition of BRDFs is usually an expensive task; it is time consuming and large memory space is required to store a database at high resolution. Thus, the dimensionality reduction of a data set of acquired BRDFs has been studied by researchers in order to keep this set at high resolution while obtaining a more compact representation.

Linear decomposition is an approach that can be used to reduce the dimensionality of a data set. The application of this technique can be seen in Weistroffer et al. [12], who used linear decomposition to perform basis decomposition from a set of scattered measurements, presenting an efficient method to decompose a data set. Following a different approach, Kautz and McCool [15] used the singular value decomposition (SVD) to decompose each BRDF and used it on interactive rendering.

The linear decomposition provides a space of BRDFs with low dimensionality. Matusik et al. [5] present an approach to generate isotropic BRDFs based on reflectance measurements. They apply linear and nonlinear dimensionality reduction and use the generated space to create new BRDFs through interpolation. In the linear and nonlinear approaches, respectively Principal Component Analysis (PCA) and Charting [16] were used.

Nielsen et al. [17] present a method to rebuild an acquired BRDF that is similar to the data-driven approach presented by Matusik et al. [5], but differs in the fact that it requires a smaller amount of measurements. The reconstruction of the BRDF data is based on the principal components from a acquired BRDF basis. The basis is pre-processed using a log-relative mapping and PCA is applied, considering a predefined set of samples. They show BRDF slices generated from the first 5 principal components of the resulting basis, where they observed that the contribution of each component represent a feature of the BRDF: specular peak, diffuse region, specular shape, Fresnel factor, and Fresnel factor with shape.

Serrano et al. [18] are also inspired by the approach proposed by Matusik et al. [5]. Their work extends Matusik's database in order to create 306 new BRDFs. To this end, PCA is used to project the convex hull of 94 BRDFs measured by Matusik in a space with five dimensions. A sampling technique approximates a uniform distribution within the convex hull. Novel BRDFs are synthesized inside the polytope defined by the 5D convex hull as a convex combination of the three nearest original MERL BRDFs. Using this extended set of 400 materials, perceptual attributes rated by users guide the creation of networks of radial basis functions. These networks are then able to map the perceptual ratings of each attribute to the underlying principal component basis coefficients of a PCA-based representation.

III. Creating New Materials through Interpolation

A new tabular representation of a BRDF can be obtained through the interpolation of a basis of materials. We apply linear decomposition using PCA in the MERL isotropic BRDF database aiming to generate a space of materials, represented by tabular representations of BRDFs. Authors as Matusik et al. [5], Nielsen et al. [17] and Serrano et al. [18] also presented similar approaches to create new materials. Following a different path, this paper applies PCA in all 100 materials from MERL database. After the PCA, Delaunay triangulation is performed and the barycentric coordinates generated from triangulation are used to interpolate materials in the original space.

A. Principal Components Analysis

Principal Components Analysis (PCA) is a technique that aims to linearly reduce the dimensionality of a data set. This method calculates the matrix of covariance from input data, as well as their associated eigenvalues and eigenvectors. This way, considering the dimension D of this data set, containing an Euclidean space with D dimensions, PCA searches k orthonormal vectors in $\mathbb{R}^D$ that better represent the data set with $k \leq D$ producing minimum square error [19].

The MERL BRDF database contains 100 different isotropic materials acquired by Matusik et al. [5]. As each material contain 3 channels (red, green and blue), 3 matrices were created representing each channel with dimension $\mathbb{R}^{N \times p}$, where $N = 100$ represents the number of materials, $p = 90 \times 90 \times 180 = 1,458,000$ is the number of samples for each material, and each row of theses matrices represent a material as a vector in $\mathbb{R}^p$. The PCA was applied in the transpose of these matrices individually in the following way.

Determine the centroid C by:

$$C = \frac{1}{N} \sum_{i=1}^{N} p_i. \tag{1}$$

Translate the origin of the coordinate system to point C:

$$u_i = p_i - C. \tag{2}$$

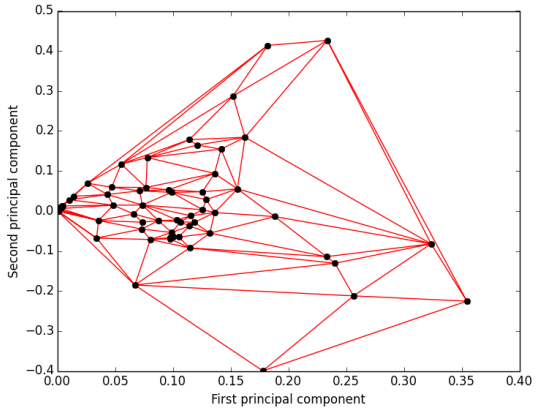

Fig. 2. Application of Delaunay triangulation in 100 materials from MERL BRDF database. Each two-dimensional point represents a material that resulted from the application of the PCA in this database. The triangulation is applied in the three channels; this figure illustrates the results for the red channel.

Calculate the covariance matrix:

$$R = \sum_{i=1}^{N} u_i u_i^T. \tag{3}$$

The eigenvalues are then arranged in descending order and their respective eigenvectors are used to construct a base β obeying that order. The eigenvectors of the base $\beta = \{v_1, v_2, \ldots, v_D\}$ are called *principal components*. Thus, to select the most significant k components ($k \leq D$), it is enough to take the first k eigenvectors of the base β, that is, $\beta_k = \{v_1, v_2, \ldots, v_k\}$, so it is possible to represent the projected data in the space generated by β_k [19], [20].

B. Triangulation

The triangulation Γ transforms a set of points on the plan into a coherent set of triangles through the attribution of a set of edges between these points. However, there can not be two crossed edges and if a new edge is added to the set, it would not cross another edge in the set [21]. In general, a triangulation creates a convex hull from the data and is composed of simplexes $\sigma_j = [p_{j_1}, p_{j_2}, \ldots, p_{j_{k+1}}]$, where each p_{j_i} is a different point, with $i = 1, \ldots, k+1$ representing a vertex of a simplex σ_j. In the case which the points are three-dimensional, the simplexes are tetrahedron. For dimension larger than three the simplexes are called by polytopes.

An important triangulation technique is called Delaunay triangulation. This technique provides a triangulation with fat angles maximizing the smallest angle of all internal angles of the resulting mesh [22]. Figure 2 shows the application of Delaunay triangulation in the MERL BRDF database. For more details about this technique refer to Janke [21] and Figueredo and Carvalho [22].

C. Barycentric Coordinates

The barycentric coordinates are weights whose sum must be 1 and each of them must have real value between 0 and 1.

TABLE I
MEAN RELATIVE ERROR FOR RECONSTRUCTION OF THE MERL BRDF DATABASE USING DIFFERENT NUMBERS OF PRINCIPAL COMPONENTS.

Number of components	Mean relative error
3	0.211647
5	0.152568
15	0.063301
30	0.027881
36	0.019620
45	0.010056

Thus, to find the value of a intermediate point p added in the simplex $\sigma_j = [p_{j_1}, p_{j_2}, \ldots, p_{j_{k+1}}]$, we will have:

$$\begin{aligned} p &= \sum_{i=1}^{k+1} \alpha_i \, p_{j_i}, \\ \sum_{i=1}^{k+1} \alpha_i &= 1 \;\text{ and }\; 0 \leq \alpha_i \leq 1, \end{aligned} \tag{4}$$

where $(\alpha_1, \alpha_2, \ldots, \alpha_{k+1})$ are the barycentric coordinates of point p.

D. Interpolation of Tabulated Materials

New tabulated materials are obtained through the interpolation of existing tabulated materials. To reach this goal, a set of 100 materials from MERL BRDF database is used, but our approach extends to any database. A new material results from the combination of all techniques previously presented in this section.

When the PCA is applied in this basis, the most significant eigenvalues and their respective eigenvectors are chosen, i.e. the principal components are selected to represent the data. It this way a reduced space is obtained without loss of relevant data. Figure 3 shows the number of components needed to select the most significant eigenvalues to construct the basis. Notice that with only 36 components, eigenvalues with values less than 0.001 for the three channels are obtained, meaning that remaining eigenvalues have little contribution to the basis. Furthermore, the mean relative error for reconstruction of this basis with 36 components is equivalent to 0.019620 (see Table I).

By applying the Delaunay triangulation in this reduced space, any new material added to this space can be created through the interpolation of materials in the original space (original basis). The triangulation provides a facility to find barycentric coordinates in this reduced space that will be used to interpolate the materials.

Figure 4a exemplifies the application of this technique on a set of materials. The dimension of the original space is represented by D and the reduced space dimension is represented by d. In this example, given a new material $\tilde{p} \subset \tilde{\sigma_j} \in \mathbb{R}^d$, it has barycentric coordinates from simplex $\tilde{\sigma_j} = [\tilde{p_1}, \tilde{p_2}, \tilde{p_3}]$. Thus,

$$\begin{aligned} \tilde{p} &= \alpha_1 \tilde{p_1} + \alpha_2 \tilde{p_2} + \alpha_3 \tilde{p_3}, \\ \alpha_1 + \alpha_2 + \alpha_3 &= 1 \;\text{ and }\; 0 \leq \alpha_i \leq 1. \end{aligned} \tag{5}$$

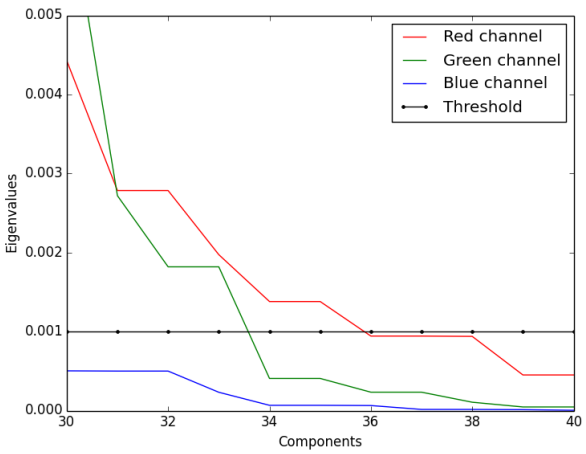

Fig. 3. Plot of the most significant eigenvalues resulting from the application of PCA using 1 to 100 components. The range from 30 to 40 illustrates the link between the eigenvalues and the mean errors relative to 1% and 2% (see Table I).

These barycentric coordinates are used to reconstruct the material $p \in \mathbb{R}^D$ through simplex $\sigma_j = [p_1, p_2, p_3]$ in the original space, such that $p = \alpha_1 p_1 + \alpha_2 p_2 + \alpha_3 p_3$.

E. Navigation Strategy

The reduced space can be navigated, and using this reflectance model a wide range of different materials are provided. This navigation can be made from one material of the basis to another. Thus, assume materials $\tilde{p}$ and $\tilde{q}$ form a segment connecting one material to another inside of the convex hull. Here, the intermediate materials $\tilde{s}(t)$ are created based on the parametric line equation:

$$\tilde{s}(t) = (1-t)\tilde{p} + \tilde{q}t, \tag{6}$$

where $t \in \mathbb{R}$ and $0 \leq t \leq 1$. Then, each intermediate material is reconstructed. Figure 4b illustrates a navigation inside a set of materials. The two materials are represented by $\tilde{p}$ and $\tilde{q}$ and their intermediated materials are represented by $\tilde{s_1}, \tilde{s_2}$ and $\tilde{s_3}$, where each $s_r = s(t_r)$ and $0 \leq t_r \leq 1$, $r = 1, 2, 3$. In the original space the navigation is linear by parts while in the reduced space the navigation is only linear. We search for the simplex $\tilde{\sigma}_j$ of the triangulation Γ which contains the intermediate points $\tilde{s}(t)$ of Equation 6. We determine the barycentric coordinates of the point $\tilde{s}(t)$ within $\tilde{\sigma}_j$, that is, $\tilde{s}(t) = (\alpha_1, \alpha_2, \alpha_3)$ and then use these coordinates for the reconstruction:

$$s(t) = \alpha_1 s_1 + \alpha_2 s_2 + \alpha_3 s_3.$$

Furthermore, notice that in the original space the triangles (simplexes) are formed only from materials that contribute in the interpolation while in the reduced space the triangles (simplexes) appear throughout the basis.

In the general case, the navigation is made for any amount of intermediate materials, that is, for two materials represented by $\tilde{p}$ and $\tilde{q}$, the intermediated materials are $\tilde{s_1}, \tilde{s_2}, \ldots, \tilde{s_r}$, with $s_r = s(t_r)$ and $0 \leq t_r \leq 1$, $r = 1, \ldots, w$, where w represent the amount of intermediate materials. Thus, using barycentric coordinates from the simplex σ_j of the triangulation Γ that contain the intermediate material $\tilde{s}(t)$, that are $\alpha_1, \ldots, \alpha_{k+1}$, the reconstruction using these coordinates is given as following:

$$\begin{aligned} s(t) &= \sum_{i=1}^{k+1} \alpha_i \, s_i, \\ \sum_{i=1}^{k+1} \alpha_i &= 1 \;\text{ and }\; 0 \leq \alpha_i \leq 1. \end{aligned} \tag{7}$$

Thus, any material is calculated using this general case (Equation 7).

IV. Results

Our linear dimensionality reduction approach was applied in the MERL BRDF database [5]. Here, we perform a navigation in this basis using three pairs of materials, each pair defining a starting and an ending material, respectively: cherry-235 and tungsten-carbide; light-brown-fabric and blue-fabric; and alum-bronze and color-changing-paint2. Each new material obtained through this navigation takes an average time of 2 minutes and 67 seconds to be generated, and about 19 minutes to be rendered. All the renderings were made using the second version of the pbrt rendering system [23]. The experiments were performed in a desktop computer with a processor Intel Core i3-4130 CPU @ 3.40GHz x 4, 4GB RAM, and Intel Haswell graphics.

Using blue-fabric and light-brown-fabric a smooth transition was made through the navigation in the reduced space. PCA was applied in this basis using only 3 principal components. Figure 5 shows this navigation through the rendering of teapots using these materials under high dynamic range environment lighting (Galileo's Tomb). The softness illustrates that this transition is coherent, indicating a valid navigation. A total of 51 tabular BRDFs were generated from our approach, including the reconstruction of the two original ones. Thus, this navigation provides 49 new materials.

In addition, this same experiment was made using two specular materials: alum-bronze and color-changing-paint2 (Figure 6). Notice that a smooth transition is also present, and specularity is consistent between the transition from one to another. Furthermore, using only 6 intermediate materials it is possible to make a smooth transition, illustrating that our navigation is also coherent for specular materials. When all 51 materials are analyzed, small details can be perceived during all the transition between renderings. A video that contains the illustration of these two experiments and a comparison between the our technique and a linear interpolation is available in https://youtu.be/nQCvL9wPI2s.

The navigation between two materials that are far from each other generates abrupt change. In this way, more intermediate materials are necessary to provide softness in the transition. Figure 7 illustrates the transition from cherry-235 to tungsten-carbide. Notice that, starting from cherry-235, when few

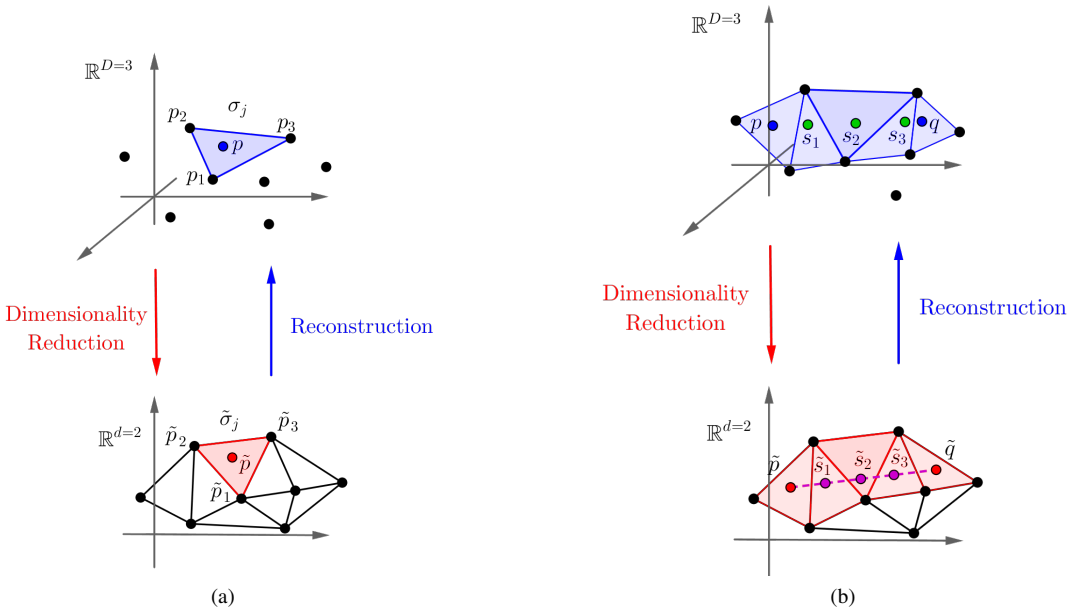

Fig. 4. Creation of new tabulated materials. (a) A new material p is created through the interpolation of existing materials. (b) Navigation in a set of materials. The new materials $\tilde{s_1}, \tilde{s_2}$ and $\tilde{s_3}$ are defined in the reduced space from the materials $\tilde{p}$ and $\tilde{q}$. They are reconstructed in the original space and are represented by s_1, s_2 and s_3 in this space.

intermediate materials are reconstructed the transition is abrupt (Figures 7a - 7f). This can be improved through the use of more intermediate materials, i.e. an interval of t that contain more points. For example, Figures 7g - 7l show a smoother transition, using $t = [0.0001, 0.0002, \ldots, 0.9999, 1]$.

To illustrate one of the contributions of our approach, Figure 8 shows a rendering of a complex scene using the Dragon model, high dynamic range environment light and three new tabular BRDFs obtained from the transition between cherry-235 and tungsten-carbide.

V. Conclusions

We present a technique to create new materials from a basis of tabular representation of BRDFs without the need of new measurements. It provides an increase in variety of materials, providing valid and coherent tabular BRDFs.

We present a compact representation of tabular BRDFs through the application of the PCA in the basis of BRDFs. Moreover, we show how to use the number of principal components to obtain a representation of the basis with respect to their eigenvalues. In this context, we show that with 36 components we can represent the MERL BRDF database, and that the remaining components dot not have significant contribution. We also show that with 36 components a mean relative error of 0.019620 is produced during the reconstruction of the basis.

Using the PCA with only 3 principal components, barycentric coordinates and Delaunay triangulation, we developed a navigation method that provides different tabular BRDFs based on the transition between two materials. In addition, we show that the transition from one to another is coherent and smooth for both matte and glossy materials. We also show one of the possible applications of our approach, using some of our new materials in a rendering of a complex scene and yielding a coherent result.

As future work, we hope to extend our model to anisotropic materials. Furthermore, we intend to improve Equation 6 so that navigation can be reparametrized on criteria inherent to the data.

Acknowledgment

The authors would like to thank the Coordination of Research from the Universidade Federal de Sergipe (COPES-UFS) due to its support through the project PVB4788-2016.

References

[1] T. Weyrich, J. Lawrence, H. P. A. Lensch, S. Rusinkiewicz, and T. Zickler, "Principles of Appearance Acquisition and Representation," *Found. Trends. Comput. Graph. Vis.*, vol. 4, no. 2, pp. 75–191, Feb. 2009.

[2] J. J. Hsia and J. C. Richmond, "A High Resolution Laser Bidirectional Reflectometer With Results on Several Optical Coatings," in *National Bureau of Standards*, Feb 1976, pp. 189–205.

[3] D. R. White, P. Saunders, S. J. Bonsey, J. van de Ven, and H. Edgar, "Reflectometer for Measuring the Bidirectional Reflectance of Rough Surfaces," *Appl. Opt.*, vol. 37, no. 16, pp. 3450–3454, 1998.

[4] S. R. Marschner, S. H. Westin, E. P. F. Lafortune, and K. E. Torrance, "Image-based bidirectional reflectance distribution function measurement," *Appl. Opt.*, vol. 39, no. 16, pp. 2592–2600, Jun 2000.

[5] W. Matusik, H. Pfister, M. Brand, and L. McMillan, "A Data-driven Reflectance Model," *ACM Trans. Graph.*, vol. 22, no. 3, pp. 759–769, Jul. 2003.

[6] R. L. Cook and K. E. Torrance, "A Reflectance Model for Computer Graphics," *ACM Trans. Graph.*, vol. 1, no. 1, pp. 7–24, Jan. 1982.

[7] X. D. He, K. E. Torrance, F. X. Sillion, and D. P. Greenberg, "A Comprehensive Physical Model for Light Reflection," in *Proceedings of the 18th Annual Conference on Computer Graphics and Interactive Techniques*, ser. SIGGRAPH '91. ACM, 1991, pp. 175–186.

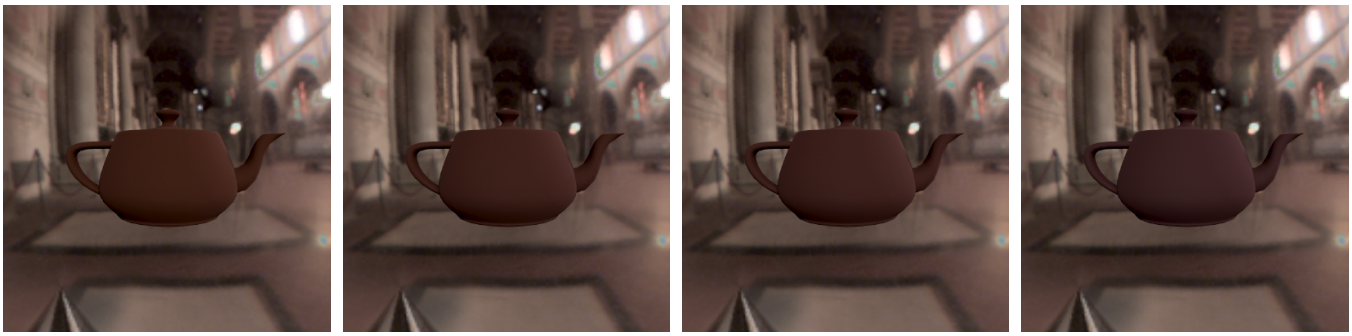

(a) $t = 0.00$ (b) $t = 0.06$ (c) $t = 0.10$ (d) $t = 0.20$

(e) $t = 0.28$ (f) $t = 0.42$ (g) $t = 0.50$ (h) $t = 0.56$

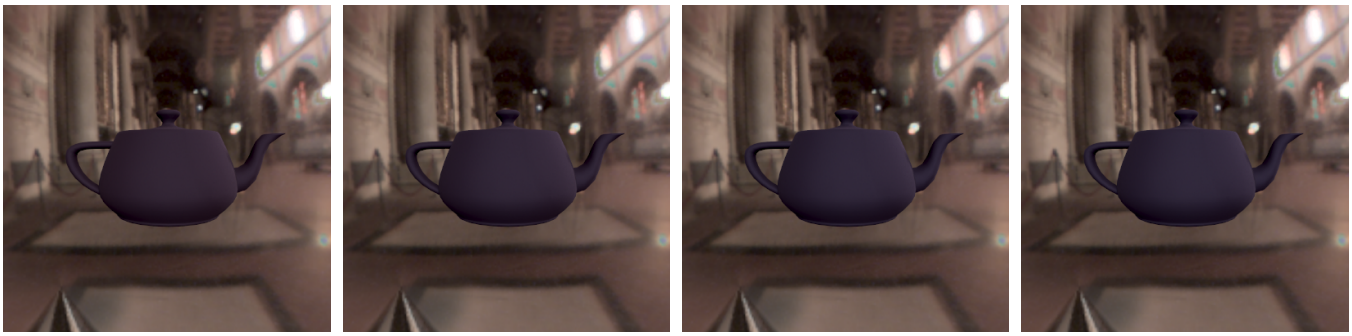

(i) $t = 0.62$ (j) $t = 0.70$ (k) $t = 0.76$ (l) $t = 0.78$

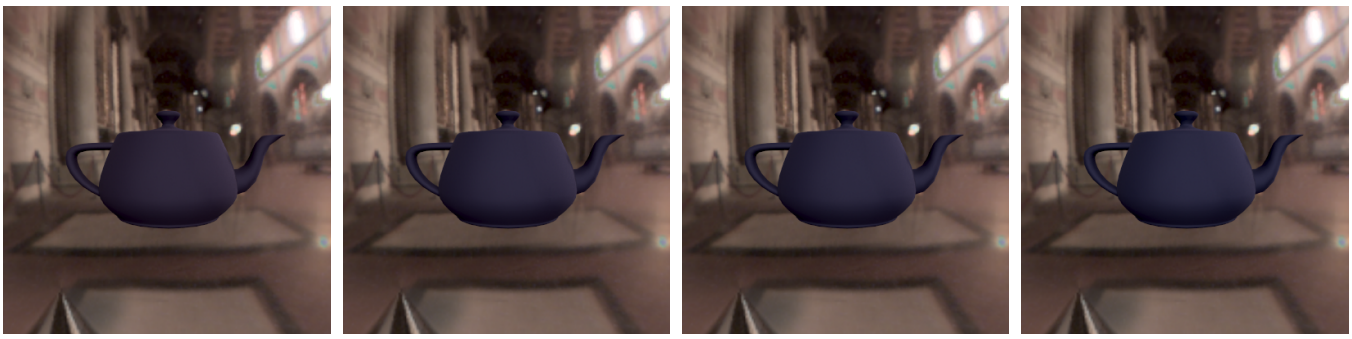

(m) $t = 0.80$ (n) $t = 0.90$ (o) $t = 0.94$ (p) $t = 1.00$

Fig. 5. Navigation using light-brown-fabric and blue-fabric materials. A total of 51 materials were obtained. The first image is a rendering of the reconstructed light-brown-fabric and the last is a rendering of the reconstructed blue-fabric. For the remaining images, intermediate materials were used in order to make a smooth transition. Notice that with only 14 intermediate materials it is already possible to show the transition from one material to another.

[8] X. D. He, P. O. Heynen, R. L. Phillips, K. E. Torrance, D. H. Salesin, and D. P. Greenberg, "A Fast and Accurate Light Reflection Model," in *Proceedings of the 19th Annual Conference on Computer Graphics and Interactive Techniques*, ser. SIGGRAPH '92, 1992, pp. 253–254.

[9] B. T. Phong, "Illumination for Computer Generated Pictures," *Commun. ACM*, vol. 18, no. 6, pp. 311–317, Jun. 1975.

(a) $t = 0.00$ (b) $t = 0.06$ (c) $t = 0.20$ (d) $t = 0.40$

(e) $t = 0.60$ (f) $t = 0.80$ (g) $t = 0.94$ (h) $t = 1.00$

Fig. 6. Navigation using two specular materials. Navigation starts from the reconstructed alum-bronze (first image) and ends on the reconstructed color-changing-paint2 (last image). The new specular materials estimated using our approach are between them. Notice that the softness is well represented with only 6 of 49 intermediate materials, and that the specularity is consistent.

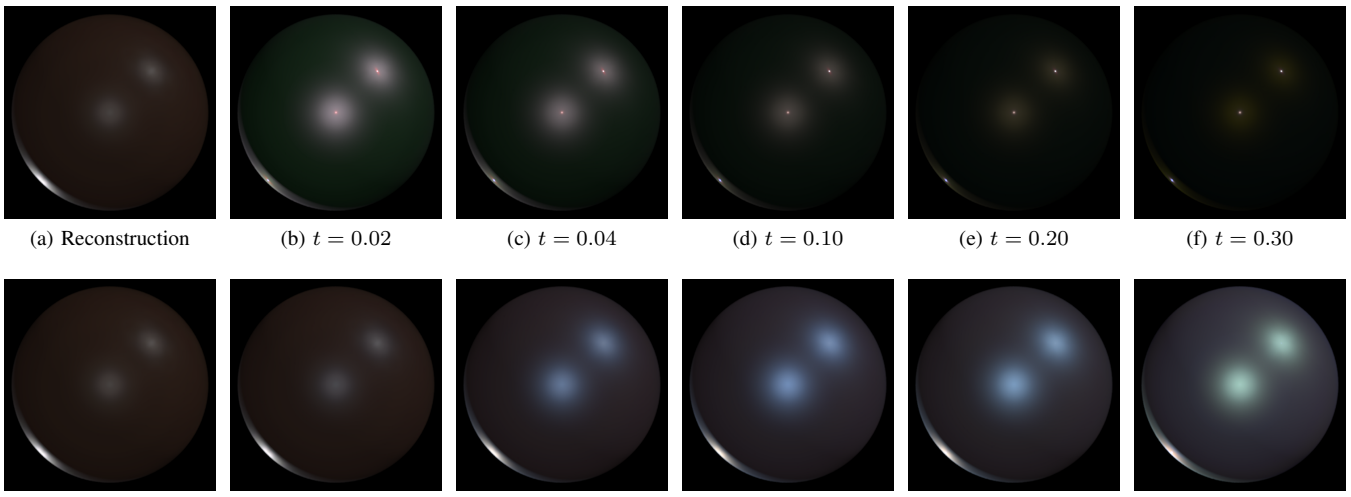

(a) Reconstruction (b) $t = 0.02$ (c) $t = 0.04$ (d) $t = 0.10$ (e) $t = 0.20$ (f) $t = 0.30$

(g) Reconstruction (h) $t = 0.0001$ (i) $t = 0.0005$ (j) $t = 0.0008$ (k) $t = 0.0010$ (l) $t = 0.0020$

Fig. 7. Spheres rendered using three points of light and composed of materials resulting from the navigation between cherry-235 and tungsten-carbide. The images in the first column represent the same rendering of the reconstructed cherry-235. The first row shows materials generated during the navigation from cherry-235 using larger transitions. As cherry-235 and tungsten-carbide are far from each other, a smoother transition can be obtained through a navigation with smaller differences between the values of t, as shown in the second row.

[10] E. P. F. Lafortune, S.-C. Foo, K. E. Torrance, and D. P. Greenberg, "Non-linear Approximation of Reflectance Functions," in *Proceedings of the 24th Annual Conference on Computer Graphics and Interactive Techniques*, ser. SIGGRAPH '97, 1997, pp. 117–126.

[11] H. P. A. Lensch, "Efficient, Image-Based Appearance Acquisition of Real-World Objects," Doctoral dissertation, Universität des Saarlandes, 2003.

[12] R. P. Weistroffer, K. R. Walcott, G. Humphreys, and J. Lawrence, "Efficient Basis Decomposition for Scattered Reflectance Data," in *Proceedings of the 18th Eurographics Conference on Rendering Techniques*, ser. EGSR'07, 2007, pp. 207–218.

[13] B. T. Andrade de Carvalho, "Image-Based Appearance Preservation," Ph.D. dissertation, Universidade Federal do Paraná, 2013.

[14] W. Matusik, H. Pfister, M. Brand, and L. McMillan, "Efficient Isotropic

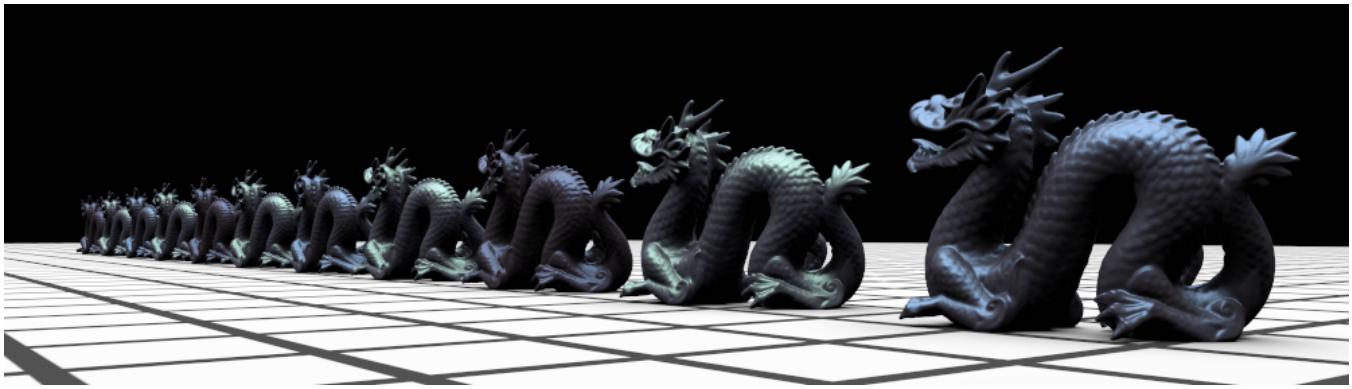

Fig. 8. Rendering from pbrt scene repository [23] using three new materials obtained using our approach. The materials were generated through the navigation between cherry-235 and tungsten-carbide. The parameter t used for these materials corresponds to the ones showed in the Figures 7i, 7k and 7l.

BRDF Measurement," in *Proceedings of the 14th Eurographics Workshop on Rendering*, ser. EGRW '03, 2003.

[15] J. Kautz and M. D. McCool, "Interactive Rendering with Arbitrary BRDFs using Separable Approximations," in *Eurographics Workshop on Rendering*. The Eurographics Association, 1999.

[16] M. Brand, "Charting a manifold," in *Advances in Neural Information Processing Systems 15*. MIT Press, 2003, pp. 961–968.

[17] J. B. Nielsen, H. W. Jensen, and R. Ramamoorthi, "On Optimal, Minimal BRDF Sampling for Reflectance Acquisition," *ACM Trans. Graph.*, vol. 34, no. 6, pp. 186:1–186:11, Oct. 2015.

[18] A. Serrano, D. Gutierrez, K. Myszkowski, H.-P. Seidel, and B. Masia, "An intuitive control space for material appearance," *ACM Trans. Graph.*, vol. 35, no. 6, pp. 186:1–186:12, Nov. 2016.

[19] G. F. Miranda Jr, G. Giraldi, C. E. Thomaz, and D. Millàn, "Composition of local normal coordinates and polyhedral geometry in riemannian manifold learning," *International Journal of Natural Computing Research (IJNCR)*, vol. 5, no. 2, pp. 37–68, 2015.

[20] I. T. Jolliffe, *Principal Component Analysis*, ser. Springer Series in Statistics. Springer, 2002.

[21] S. J. Janke, *Mathematical Structures for Computer Graphics*. New York, NY, USA: John Wiley & Sons, Inc., 2015.

[22] L. H. de Figueiredo and P. C. P. Carvalho, *Introdução à geometria computacional*, ser. Annals of discrete mathematics. Conselho Nacional de Desenvolvimento Cientifico e Tecnologico, May 1991.

[23] W. J. Matt Pharr and G. Humphreys., "pbrt rendering system, version 2." Feb 2016.